

Synthesis of Hydroxyapatite-Zirconia Composite and Activity Test as Dental Implant Material

Atiek Rostika Noviyanti^{1*}, Difa Muhammad Yashfi¹, Yusi Deawati¹, Eneng Maryani², Sabila Aulia Hemzah¹, Azman Ma'amor³

¹Department of Chemistry, Faculty of Mathematics and Natural Sciences, Universitas Padjadjaran, Sumedang, 45363, West Java, Indonesia

²Center for Standardization and Textile Industry Services, Jl. A. Yani No.392, Kebonwaru, Batununggal District, Bandung City, 40272, West Java, Indonesia

³Chemistry Department, Faculty of Science, Universiti Malaya, 50603 Kuala Lumpur, Wilayah Persekutuan Kuala Lumpur, Malaysia

*Corresponding author: atiek.noviyanti@unpad.ac.id

DOI: <https://doi.org/10.24198/cna.v13.n1.60026>

Abstract: Hydroxyapatite (HAp) is one of the bioceramics that is widely used in various fields, one of which is the health sector as a dental implant material. One of the reasons is that hydroxyapatite has good biocompatibility. In this study, natural calcium sources such as eggshell waste were utilized for the synthesis of hydroxyapatite. However, its mechanical properties do not yet meet the requirements as a dental implant material, its modification is usually done by adding other compounds, such as zirconium oxide. Zirconium oxide can be used as a support material because it has good strength, toughness, and durability as a dental implant. Therefore, in this study, a hydroxyapatite-zirconium oxide (HAp-ZrO₂) composite was synthesized for dental implant material. This study aims to determine the effect of adding ZrO₂ on increasing the mechanical and corrosion resistance of HAp. The research methods include isolation of CaO from chicken eggshells, synthesis of hydroxyapatite, synthesis of HAp-ZrO₂ composite, hardness test, and corrosion resistance test. Based on SEM images, the addition of ZrO₂ can reduce the level of HAp agglomeration. The addition of ZrO₂ to HAp did not significantly affect the increase in HAp hardness since the zirconia phase formed is possibly dominated by the cubic phase. The optimum HAp-ZrO₂ composite was obtained with a variation of HAp-90%-ZrO₂-10% which showed the highest crystallinity of 75.37% with a crystal size at 10.15 nm with corrosion resistance comparable to pure HAp.

Keywords: composites, dental implants, hydroxyapatite, zirconia

Abstrak: Hidroksiapatit (HAp) adalah salah satu jenis biokeramik yang banyak digunakan di berbagai bidang, salah satunya di bidang kesehatan sebagai bahan implan gigi. Salah satu alasan penggunaannya adalah karena hidroksiapatit memiliki biokompatibilitas yang baik. Dalam penelitian ini, sumber kalsium alami seperti limbah cangkang telur dimanfaatkan untuk sintesis hidroksiapatit. Namun, sifat mekaniknya belum memenuhi persyaratan sebagai bahan implan gigi, sehingga modifikasi biasanya dilakukan dengan menambahkan senyawa lain, seperti zirkonium oksida. Zirkonium oksida dapat digunakan sebagai bahan pendukung karena memiliki kekuatan, ketangguhan, dan daya tahan yang baik sebagai bahan implan gigi. Oleh karena itu, dalam penelitian ini disintesis komposit hidroksiapatit-zirkonium oksida (HAp-ZrO₂) sebagai bahan implan gigi. Penelitian ini bertujuan untuk mengetahui pengaruh penambahan ZrO₂ terhadap peningkatan sifat mekanik dan ketahanan korosi HAp. Metode penelitian meliputi isolasi CaO dari cangkang telur ayam, sintesis hidroksiapatit, sintesis komposit HAp-ZrO₂, uji kekerasan, dan uji ketahanan korosi. Berdasarkan citra SEM, penambahan ZrO₂ dapat mengurangi tingkat aglomerasi HAp. Penambahan ZrO₂ pada HAp tidak memberikan pengaruh signifikan terhadap peningkatan kekerasan HAp, karena kemungkinan fase zirkonia yang terbentuk didominasi oleh fase kubik. Komposit HAp-ZrO₂ yang optimum diperoleh pada variasi HAp 90% - ZrO₂ 10%, yang menunjukkan tingkat kristalinitas tertinggi sebesar 75,37% dengan ukuran kristal 10,15 nm serta ketahanan korosi yang sebanding dengan HAp murni.

Kata kunci: komposit, implan gigi, hidroksiapatit, zirkonia

INTRODUCTION

Currently, bioceramics are widely used in various fields because of their usefulness for several applications. Bioceramics are synthetic prostheses of ceramics that are widely used for biological purposes such as materials for knees, hips, and teeth. Bioceramics are made with high absorption and can regenerate natural bone or tooth tissue throughout human tissue and can withstand sufficient loads. Most bioceramics are based on calcium phosphate, especially hydroxyapatite (HAp) (Veluswamy *et al.* 2024). Currently, the development of bioceramics is being carried out which are useful for dental or bone implants with sufficient strength by using nano-structured HAp with very large coverage. One of the bioceramics used is a hydroxyapatite-zirconia composite as a material for dental implants.

HAp ($\text{Ca}_{10}(\text{PO}_4)_6(\text{OH})_2$) is a small part of human bone and tooth material HAp can help bone and tooth growth without using fibrous tissue. Hydroxyapatite shows excellent biocompatibility with natural hard and soft tissues in teeth). Therefore, hydroxyapatite is very suitable for use as a dental implant because of its good biocompatibility and also good bone and tissue bonding ability (Noviyanti *et al.* 2020). Hydroxyapatite can be sourced from natural materials as a source of calcium such as coral (Mohan *et al.* 2018) seaweed, (El-Said *et al.* 2024) and chicken eggshells (Noviyanti *et al.* 2020). Chicken eggshells are one of the natural materials that easy to use and currently chicken eggshells are a fairly serious waste problem. It was reported that, chicken eggshell waste reaches 136.956 tons annually. The calcium content in chicken eggshells reaches 94% which makes it one of the promising natural materials to be a source of calcium in the synthesis of HAp (Noviyanti *et al.* 2020). Hydroxyapatite can be synthesized through several methods such as the solid phase reaction method (Mobarak *et al.* 2024), precipitation (Zheng *et al.* 2024) and hydrothermal (Noviyanti *et al.* 2020). The use of the hydrothermal method is widely used in synthesizing HAp, because the method produces high crystallinity material. In addition, this method provided several advantages such as economical costs, short reaction stages, use of low temperatures during synthesis, and environmentally friendly.

Zirconia (zirconium oxide, ZrO_2) is a material that has optimal properties for dental implant use due to its toughness, strength, and durability, as well as excellent wear properties. Therefore, zirconium oxide has good biocompatibility material (Kumar *et al.* 2024). Zirconium metal (Zr) is a very strong metal with chemical and physical properties similar to titanium metal (Ti). In dentistry, these two metals are commonly used as dental implant materials because they do not inhibit bone-forming cells (osteoblasts). The materials used in dental implants must have biocompatibility properties, excellent antibacterial and toxicity activity (Yılmaz & Çalışkan 2022), good stability, resistant to corrosion (Li *et al.* 2025), and

have high performance to survive in a complex oral environment (Luo *et al.* 2020). Zirconia can be synthesized via hydrothermal methods (Zhou *et al.* 2024), sol gel (Crespo *et al.* 2009), spray pyrolysis (Hwangbo & Lee 2019) coprecipitation (Li *et al.* 2020), chemical vapor synthesis (Baek *et al.* 2017) and colloidal gel methods (Septawendar *et al.* 2019).

In this study, the synthesis of HAp from chicken eggshells was carried out via hydrothermal method and the synthesis of HAp-zirconia composites using the sol gel method with PEG-6000 as a dispersant with variations of HAp-80%- ZrO_2 -20%; HAp-85%- ZrO_2 -15%; and HAp-90%- ZrO_2 -10%. In addition, the synthesized composites were tested for activity as dental implants via Vickers hardness and corrosion resistance tests. Prior to-Vickers hardness test, the samples were first sintered with sintering temperature variations of 850°C, 950°C, and 1050°C. The sintering process is the heating of the material heated below its melting point so that the metal powder will fuse together due to the mass transformation mechanism due to diffusion of atoms on the surface of the powder. The purpose of the sintering process is to form bonds between particles. In 2018, Maryani *et al.* synthesized HAp-zirconia composites with variations of HAp-25%- ZrO_2 -75%, HAp-50%- ZrO_2 -50%, and HAp-75%- ZrO_2 -25% (Maryani *et al.* 2018). The study showed that the variation of HAp 75%- ZrO_2 25% was the best variation because it was bioactive due to the highest HAp content and all zirconia crystals were observed in the tetragonal phase. Therefore, the variations of HAp-80%- ZrO_2 -20%; HAp-85%- ZrO_2 -15%; and HAp-90%- ZrO_2 -10% were used because more HAp composition in each variation.

MATERIALS AND METHODS

Materials

The research materials used were technical ammonium bicarbonate (NH_4HCO_3) from PT. Brataco Indonesia, 95-97% sulfuric acid (H_2SO_4) pa from Merck KGaA Darmstadt Germany, chicken egg shells, dihydrogen ammonium phosphate (DHP) ($\text{NH}_4(\text{H}_2\text{PO}_4)$) from Merck, PEG-6000 from PT. Brataco Indonesia, and zirconium oxyhydroxide ($\text{ZrO}(\text{OH})_2$) based on local zirconium silicate from PT. Monokem Surya Indonesia West Kalimantan.

Synthesis of Hydroxyapatite (HAp)

A total of 2.825 g of CaO isolated from chicken eggshells was added to 3.960 g of dihydrogen ammonium phosphate DHP, then dissolved in 100 mL of distilled water. The mixture was reacted hydrothermally at a temperature of 230°C for 48 hours. The solid obtained was then filtered and washed with distilled water until it reached pH 7 to remove NH_4OH and dried at 100°C for 2 hours (Noviyanti *et al.* 2020). To prove that the solid obtained was HAp, the next process was carried out

to characterize its structure and morphology using XRD and SEM, respectively.

Synthesis of Hydroxyapatite (HAp)-Zirconia (ZrO₂) Composite

Zr was obtained by dissolving zirconium oxyhydroxide in 95-97% sulfuric acid as much as 25 mL. The acidity of the zirconium oxyhydroxide solution was adjusted to pH 3 using 1 M ammonium bicarbonate (NH₄HCO₃). The resulting solution was then added to HAp with a mass ratio of 80% to zirconia and stirred until homogeneous. The same procedure was carried out for the 85 and 90% HAp variations. The three variations of the HAp-ZrO₂ composite were then added to 10% PEG-6000 with a mixed volume ratio of HAp-ZrO₂: PEG (15:1) which was done using the sol-gel method. The mixture was stirred homogeneously for 1 hour and then heated for 3 hours at a temperature of 120°C. Furthermore, the heated mixture gel was left at room temperature for 12 hours and then filtered. And dried at a temperature of 100°C for 48 hours until a solid is obtained. The solid was washed with hot water to remove impurities and re-dried at 100°C for 24 hours. The resulting HAp-ZrO₂ solid was calcined at 800°C. Then their respective structures and morphologies were characterized by XRD and SEM (Septawendar *et al.* 2019). The three composite samples are then called HAp-80%-ZrO₂-20%, HAp-85%-ZrO₂-15%, HAp-90%-ZrO₂-10%.

Mechanical Properties Testing of HAp-ZrO₂

All composite samples were tested for hardness using the Vickers Hardness Tester. Measurements were made by placing the composite samples that had been molded into a tube with a diameter of 2 cm and a height of 1 cm. Then, the mold was given a load of 200 gf for 10 seconds. The Vickers hardness value was calculated using equation (1):

$$HV = \frac{2P \sin(\theta/2)}{d^2} \dots (1)$$

with: HV = Vickers Hardness, P = Load (kgf), α = opposite angle on the indenter, and d = average indentation diagonal. It can be seen more clearly in the explanation of the Vickers test principle in Figure 1.

Mechanical Properties Testing of HAp-ZrO₂ Composites

The corrosion resistance of all composite samples was carried out using the *in vitro* biodegradation test method. Biodegradation simulation was carried out to observe the decay rate/weight loss of the samples by immersing the HAp-ZrO₂ composite pellets in a Simulated Body Fluid (SBF) solution composition which is similar to blood plasma as depicted in Table 1. The pellets were soaked in SBF solution pH 7.4 for 3 days at temperature 37°C. After 3 days, the pH of SBF were remeasured and pellets composite washed with aquadest, then dried at 70°C. To determine the weight loss, the composite was weighed until the weight was constant.

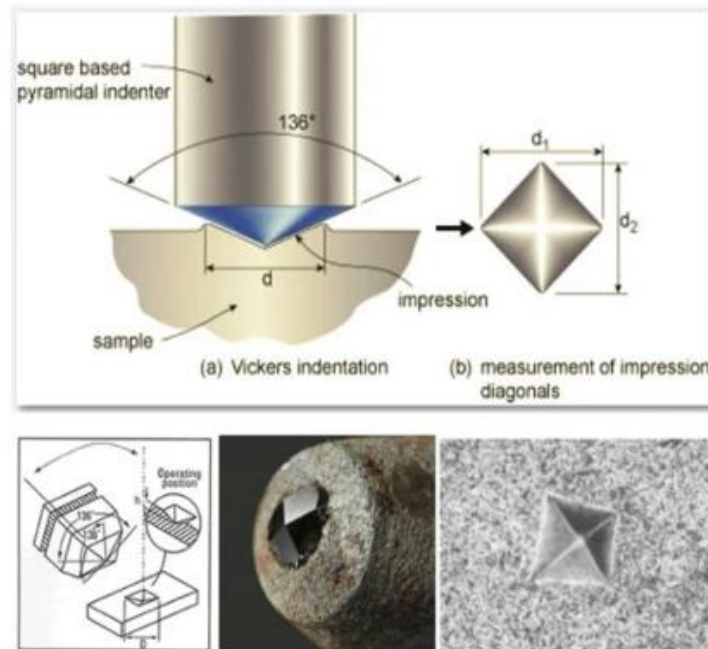


Figure. 1 Vickers test principle

Table 1. Comparison of ions in SBF and blood plasma in the human body (Kaewsichan *et al.* 2011)

Type	Ion Concentration (mM)						
	Na ⁺	K ⁺	Mg ²⁺	Ca ²⁺	Cl ⁻	HCO ₃ ⁻	HPO ₄ ²⁻
Blood plasma	142.0	5.0	1.5	2.5	103.0	27.0	1.0
SBF	142.0	5.0	1.5	2.5	148.8	4.2	1.0

RESULTS AND DISCUSSION

Determination HAp Structure

HAp structure was characterized by XRD, typical XRD diffractogram peaks for HAp are 2 θ : 25.91 $^{\circ}$; 27.67 $^{\circ}$; 31.80 $^{\circ}$; 32.21 $^{\circ}$. There is a peak with high intensity in the 2 θ region around 30 $^{\circ}$. The peaks that appear are in accordance with the diffractogram based on the crystallography open database with COD ID 2300273 as shown in Figure 2. From this analysis it can be concluded that the synthesis of HAp by the hydrothermal method has been successfully carried out. This is also supported by the lattice parameter data $a = 9.421 \text{ \AA}$; $b = 9.421 \text{ \AA}$; and $c = 6.880 \text{ \AA}$ which are in accordance with the general HAp space group. The crystal size of HAp in this study was found at 27.86 nm.

In addition to its structure data, HAp crystallinity data was also determined at 80.84% based from the XRD data. With this value, it is stated that the HAp obtained has high crystallinity.

Determination of HAp-ZrO₂ Composite Structure with XRD

Similar to the determination of HAp structure, the composite structure was also determined by XRD on all variations of composite samples of HAp-80%-ZrO₂-20%, HAp-85%-ZrO₂-15%, and HAp-90%-ZrO₂-10% after calcination at 800 $^{\circ}$ C as demonstrated in Figure 3.

There is no difference in the diffractograms of the three composites, all showing the same peak positions at 2 θ : 25.49 $^{\circ}$; 31.41 $^{\circ}$; and 36.34 $^{\circ}$. Several peaks with high intensity were found at the positions 2 θ : 25.50 $^{\circ}$, 31.50 $^{\circ}$, and 38.80 $^{\circ}$. These peaks indicate the formation of HAp-ZrO₂ composite and zirconium minerals that are often found in nature, namely ZrSiO₄ (Liu *et al.* 2016). The presence of ZrSiO₄ minerals comes from the precursor ZrO(OH)₂ which comes from zirconium silicate containing SiO₂, so that when synthesized, ZrSiO₄ is formed and affects the measurements on the HAp-ZrO₂ sample after drying at 100 $^{\circ}$ C. In the variation of the HAp-80%-ZrO₂-20% composite, the peak area 2 θ : 25.49 $^{\circ}$, 31.41 $^{\circ}$, and 38.69 $^{\circ}$ there is zirconia with a cubic phase. In the HAp-85%-ZrO₂-15% composite variation, peak areas 2 θ : 25.60 $^{\circ}$, 31.20 $^{\circ}$, and 38.75 $^{\circ}$ contain zirconia with a cubic phase. In the variation of HAp-90%-ZrO₂-10% composite peak area 2 θ : 25.53 $^{\circ}$, 31.34 $^{\circ}$, and 38.80 $^{\circ}$ there is zirconia presence with cubic phase. Based on the XRD analysis shown in Table 2, the HAp-80%-ZrO₂-20% composite

calcined at 800 $^{\circ}$ C has a crystallinity of 67.11% and a c-ZrO₂ crystallite size of 52.44 nm on the *hkl* (111) and (200) crystal planes, the HAp-85%-ZrO₂-15% composite calcined at 800 $^{\circ}$ C has a crystallinity of 51.46% and a c-ZrO₂ crystallite size of 13.81 nm on the *hkl* (111) and (200) crystal planes, and the HAp-90%-ZrO₂-10% of the 800 $^{\circ}$ C calcination results have a crystallinity of 75.37% and a c-ZrO₂ crystallite size of 10.15 nm on the *hkl* (111) and (200) crystal planes.

The average size of the composite crystal is 25 nm calculated based on the Scherrer equation. The emergence of the c-ZrO₂ phase is seen from its diffraction peak at the diffraction angle, 2 θ : 31.20 $^{\circ}$. Meanwhile, at the diffraction angle of 2 θ , from 25.45 $^{\circ}$ indicates the presence of HAp-ZrO₂ composite. After being analyzed, the 80% composite obtained a crystallinity of 67.11%; the 85% composite obtained a crystallinity of 51.46%; and the 90% composite obtained a crystallinity of 75.37%. In addition, cubic ZrO₂ crystal phase and hexagonal hydroxyapatite crystal phase were obtained.

Microstructure Analysis of HAp-ZrO₂ Composites

The effect of ZrO₂ addition on the composite microstructure was analyzed by SEM as shown in Figure 4.

Based on SEM image of hydroxyapatite, the addition of ZrO₂ is seen to reduce the particle size, thereby increasing the density of the composite particles. Likewise, the level of agglomeration decreases with the addition of ZrO₂. The use of PEG in the composite mixture is also carried out to withstand particle interactions through the interaction mechanism between the hydroxyl group (-OH) of the zirconium oxyhydroxide precursor (Zr(OH)₂ · xH₂O) with the ether group (-O-) of PEG (Septawendar & Maryani 2020). PEG plays a role in enveloping and covering the surface of the particles, thereby reducing particle agglomeration due to steric hindrance from PEG molecules. Thus, it is found that the morphology of HAp without the addition of PEG is more agglomerated compared to the morphology of all variations of the HAp-ZrO₂ composite.

Analysis of Mechanical Properties of HAp-Zirconia Composites

In this study, the mechanical properties tested were hardness (Vickers hardness). Hardness is one of the most important parameters for comparing the properties of dental implant materials. It is used to find the suitability of clinical use of biomaterials. Before testing, the samples were formed into pellets

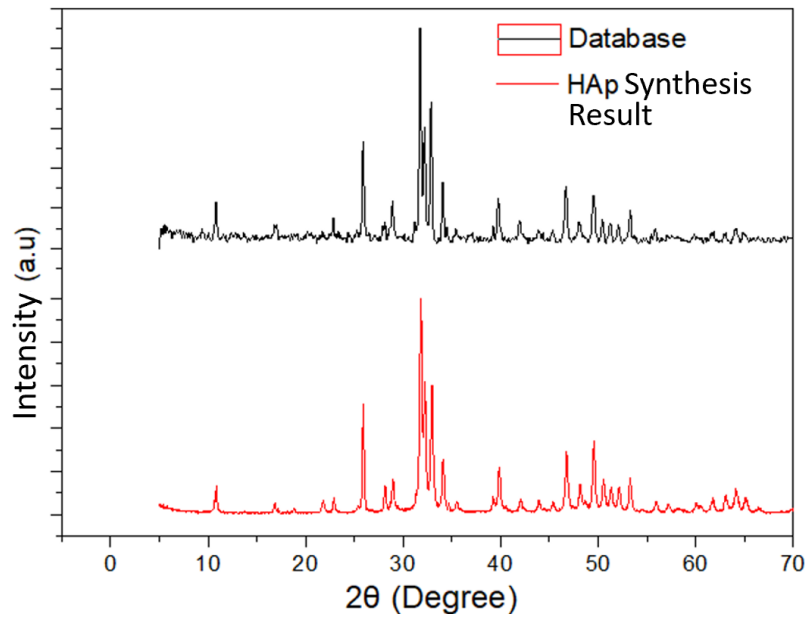


Figure 2. XRD diffractogram of HAp from synthesis and standard

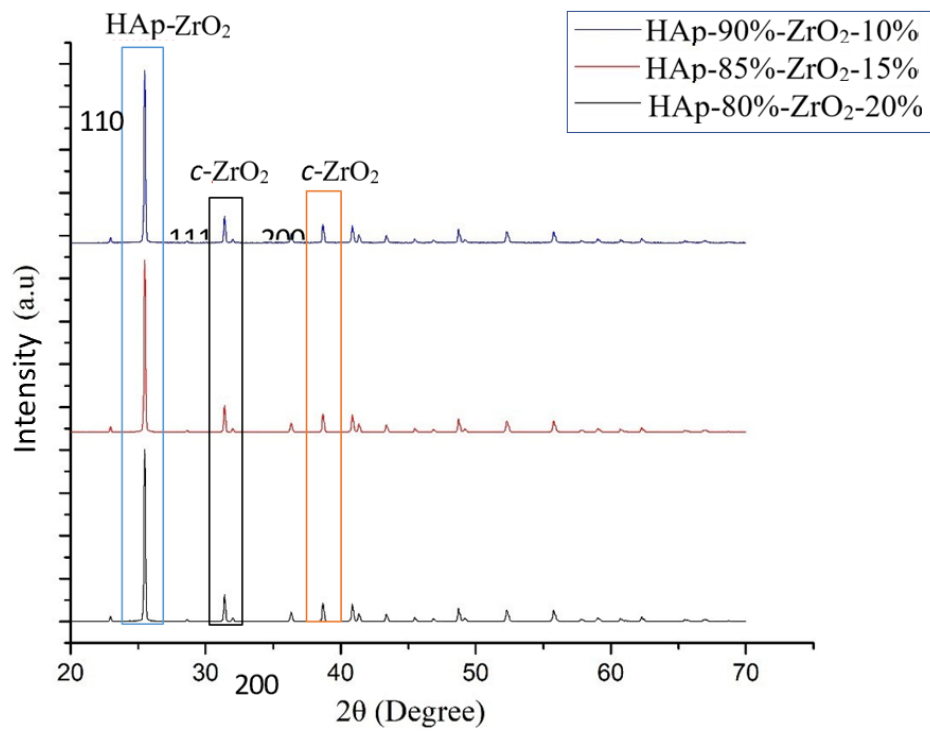


Figure 3. Comparison of XRD diffractograms of all compositions

Table 2. Crystallinity and crystallite size of HAp-ZrO₂

Sample	Crystallinity (%)	The crystallite size of <i>c</i> -ZrO ₂ (nm)
HAp-80%-ZrO ₂ -20%	67.11	52.44
HAp-85%-ZrO ₂ -15%	51.46	13.81
HAp-90%-ZrO ₂ -10%	75.37	10.15

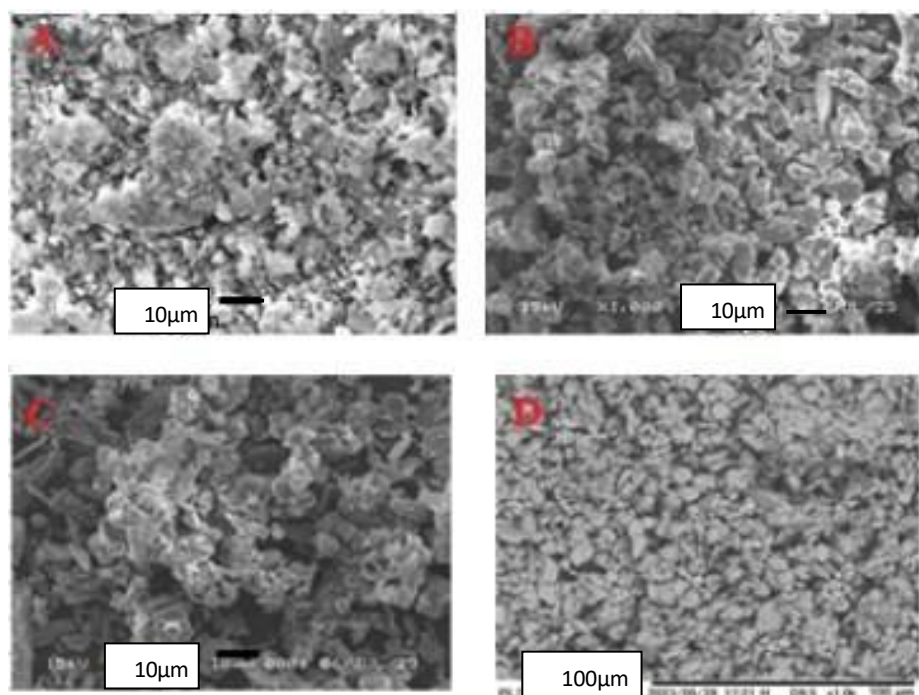


Figure 4. SEM images of (a) HAp, (b) HAp-90%-ZrO₂-10%, (c) HAp-85%-ZrO₂-15%, (d) HAp-80%-ZrO₂-20%.

first by applying pressure to the samples of 5000 Pa for 15 minutes. The results of the hardness test are shown in Table 3, Table 4, and Table 5.

The hardness test results showed that the addition of zirconia actually reduced the hardness of the composite. This is because the zirconia crystal phase formed is a cubic phase, while a tetragonal crystal phase is needed so that zirconia can increase the hardness of the composite to the maximum. In addition, the sample is suspected of being inhomogeneous which causes fluctuating data and in the Vickers hardness test and the sample surface which greatly affects the test results (Gušin *et al.* 2019). When testing is carried out, triangle the pressure results given will be very different. When an uneven or rough surface is given pressure, the pressure triangle will produce a very large distance so that this will cause the calculation of the Vickers hardness value to be small. Likewise, when the surface is flat, the pressure triangle will produce a small distance so that the calculation of the Vickers hardness value becomes large. Pure HAp has the highest hardness with a value of 464 HV or 4550 mPa at the first point and a sintering temperature of 950°C. Among the 3 composite variations, the HAp-90%-ZrO₂-10% composite variation has better hardness than the other variations. Higher sintering temperatures have been shown to increase the hardness level of the composite.

Corrosion Resistance Analysis of HAp-ZrO₂ Composites

The corrosion resistance of HAp-ZrO₂ composites

was carried out by *in vitro* biodegradation test which is useful for determining the resistance of materials immersed in SBF (Simulated Body Fluid) solution for 3 days at a temperature of 37°C. Figure 6 shows the change in pH of the SBF solution after HAp and HAp-ZrO₂ composites were immersed for 3 days.

Sample immersion for 3 days in SBF solution at 37°C showed pH changes. SBF solution without sample immersion had an initial pH of 7.40. After sample immersion for 3 days at 37°C, there was a change in the pH of the solution in HAp, HAp-80%-ZrO₂-20%, HAp-85%-ZrO₂-15%, and HAp-90%-ZrO₂-10% which can be seen in Figure 6. Significant changes occurred in the composition variation of HAp-80%-ZrO₂-20% with a pH of 8.91. Meanwhile, pH changes in the composition variations of HAp-85%-ZrO₂-15%, HAp-90%-ZrO₂-10%, and HAp occurred minimally. Meanwhile, the pH of the SBF solution left for 3 days at 37°C remained the same, which was 7.40. The pH change is thought to occur due to the release of Zr⁴⁺ ions from zirconium which can be seen from the reduction in sample mass after immersion which can be seen in Figure 7. The reaction of ZrO₂ in aqueous medium can follow the reaction equation (2):



The largest mass change after immersion in SBF solution for 3 days at 37°C occurred in the variation of HAp-80%-ZrO₂-20% with a mass loss of 14.96%. As seen in Figure 7, the degradation of the sample

Table 3. Vickers hardness level of hydroxyapatite and variations of hydroxyapatite zirconia composites synthesized at a sintering temperature of 850°C

Sample		Hardness (HV)	Hardness (mPa)
Pure HAp	Point 1	204	2001
	Point 2	225	2207
	Point 3	156	1530
HAp-90%-ZrO ₂ -10%	Point 1	150	1471
	Point 2	153	1500
	Point 3	150	1471
HAp-85%-ZrO ₂ -15%	Point 1	144	1412
	Point 2	124	1216
	Point 3	112	1098
HAp-80%-ZrO ₂ -20%	Point 1	100	980.7
	Point 2	123	1206
	Point 3	118	1157

Table 4. Levels violence Vickers hydroxyapatite and variations of hydroxyapatite-zirconia composites synthesized at a sintering temperature of 950°C

Sample		Hardness (HV)	Hardness (mPa)
Pure HAp	Point 1	464	4550
	Point 2	268	2628
	Point 3	273	2677
HAp-90%-ZrO ₂ -10%	Point 1	290	2844
	Point 2	181	1775
	Point 3	290	2844
HAp-85%-ZrO ₂ -15%	Point 1	200	1961
	Point 2	181	1795
	Point 3	192	1883
HAp-80%-ZrO ₂ -20%	Point 1	200	1961
	Point 2	176	1726
	Point 3	174	1706

Table 5. Levels violence Vickers hydroxyapatite and variations of hydroxyapatite-zirconia composites synthesized at a sintering temperature of 1050°C

Sample		Hardness (HV)	Hardness (mPa)
Pure HAp	Point 1	474	4649
	Point 2	470	4609
	Point 3	356	3491
HAp-90%-ZrO ₂ -10%	Point 1	323	3168
	Point 2	320	3138
	Point 3	302	2962
HAp-85%-ZrO ₂ -15%	Point 1	220	2158
	Point 2	213	2089
	Point 3	200	1961
HAp-80%-ZrO ₂ -20%	Point 1	205	2010
	Point 2	200	1961
	Point 3	179	1755



Figure 5. 100x magnification of Vickers micro measurement of HAp-zirconia composite.

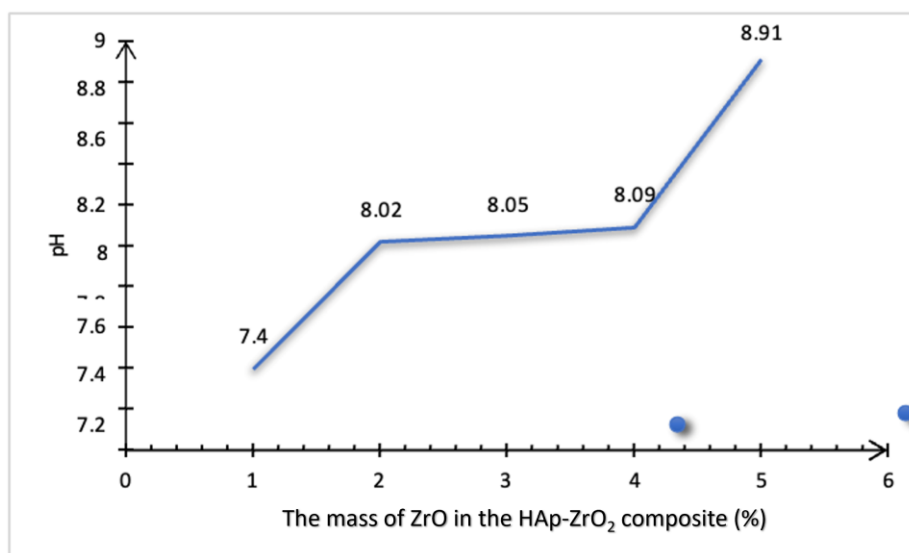


Figure 6. Effect of mass percentage of ZrO₂ on pH of SBF solution after soaking for 3 days at 37°C.

Table 6. Biodegradation of HAp-ZrO₂ composites of all variations

Sample	Initial mass (g)	Final mass (g)	Subtraction mass (%)
Pure HAp	0.447	0.437	2.23
HAp-90%-ZrO ₂ -10%	0.662	0.630	4.83
HAp-85%-ZrO ₂ -15%	0.536	0.475	11.38
HAp-80%-ZrO ₂ -20%	0.567	0.483	14.96

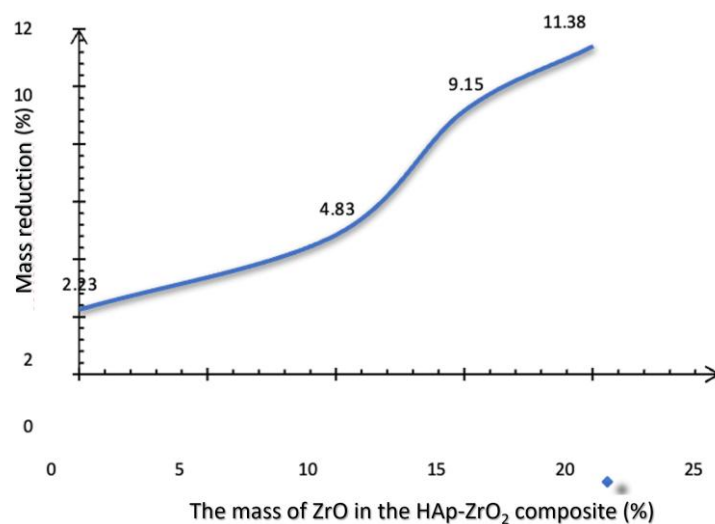


Figure 7. Mass reduction graph of *in vitro* biodegradation test

that occurred was influenced by the % mass of ZrO_2 . These data show a correlation between changes in SBF pH and the amount of ZrO_2 sample dissolved in SBF.

Based on the composition variations seen in Table 6, it can be concluded that the greater the percentage (%) mass of ZrO_2 given, the weaker the degradation resistance to SBF solution. However, in the variation of the HAp-90%- ZrO_2 -10% composite, it has similar degradation resistance to SBF with HAp. In addition, in-vivo testing is needed to determine the time of osteoblast formation in bones and the effect of pH on osteoblast cells. This is because changes in pH in the osteoblast cell environment can provide unexpected responses such as inflammation so that the formation of osteoblast cells is slow (Ghodraty *et al.* 2025).

CONCLUSION

Based on the results obtained from this study, it can be concluded that the synthesis of HAp- ZrO_2 composites using the sol gel method with PEG-6000 dispersant produces a hexagonal phase in HAp and cubic in ZrO_2 with the highest crystallinity in the HAp-90%- ZrO_2 -10% variation with a value of 75.37% and a crystal size of 10.15 nm. In addition, the results of the surface morphology of the HAp- ZrO_2 composite are better than pure HAp with minimal agglomeration caused by the role of PEG-6000 as a dispersant during synthesis. The smallest particle size was obtained in the HAp-90%- ZrO_2 -10% variation of 500 nm. In addition, the effect of the addition of ZrO_2 on the mechanical properties of the composite is fluctuating. The HAp-90%- ZrO_2 -10% variation shows the highest Vickers hardness value compared to other variations. In addition, the effect of the addition of ZrO_2 on corrosion resistance is comparable to pure HAp. In the HAp-90%- ZrO_2 -10% variation, it has corrosion resistance comparable to pure HAp, making the HAp-90%- ZrO_2 -10% variation the best variation to be used as a dental implant.

ACKNOWLEDGMENTS

The author would like to thank the Center for Ceramics for the facilities provided in this research.

Funding

Authors are grateful for Universitas Padjadjaran, Indonesia, by Hibah Riset Data Pustaka dan Daring (HRDPD) (2225/UN6.3.1/PT.00/2024) and Academic Leadership Grant (ALG) Prof. Dr. Atiek Rostika Noviyanti (ID: 1419/UN6.3.1/PT.00/2024).

Author statement

-

Declaration of competing interests

There is no conflict of interests.

REFERENCES

- Baek, M.K., Park, S.J. & Choi, D.J. (2017). Synthesis of zirconia (ZrO_2) nanowires via chemical vapor deposition. *Journal of Crystal Growth*. **459**: 198-202.
- Crespo, M.D., Murillo, A.G., Torres-Huerta, A.M., Yanez-Zamora, C. & Carrillo-Romo, F.D.J. (2009). Electrochemical behaviour of ceramic yttria stabilized zirconia on carbon steel synthesized via sol-gel process. *Journal of Alloys and Compounds*. **483(1-2)**: 437-441.
- El-Said, G.F., El Zokm, G.M., El-Sikaily, A. & Ismail, M. M. (2024). Comparison of crude nano-hydroxyapatite extracted from calcified seaweed in terms of composition, antibacterial activity, and cytotoxicity. *Environmental Nanotechnology, Monitoring & Management*. **21**: 100908.
- Ghodraty, H., Goodarzi, A., Golrokhian, M., Fattahi, F., Anzabi, R.M., Mohammadikhah, M., Sadeghi, S. & Mirhadi, S. (2025). A narrative review of recent developments in osseointegration and anti-corrosion of titanium dental implants with nano surface. *Bone Reports*. **25**:101846.
- Gušin, A.Z., Žužek, B., Podgornik, B. & Kevorkijan, V. (2019). The uncertainty of hardness measurements related to the measurement method, surface preparation and range of the measurements. *Materiali in Tehnologije*. **53(6)**: 897-904.
- Hwangbo, Y. & Lee, Y. I. (2019). Facile synthesis of zirconia nanoparticles using a salt-assisted ultrasonic spray pyrolysis combined with a citrate precursor method. *Journal of Alloys and Compounds*. **771**: 821-826.
- Kumar, K.N., Vijayalakshmi, L., Saijyothi, K., Prakash, N.G., Harisha, B.S., Ko, T.J., Ganesh, K.S., Lim, J., Karim, M.R. & Alnaser, I.A. (2024). Non-cytotoxic, biocompatible pyrochlore Cerium Zirconium Oxide nanoparticles for asymmetric supercapacitor applications. *Ceramics International*. **50(24)**: 54596-54604.
- Li, A.X., Wang, Y.L., Xiong, X., Liu, H.F., Wu, N. N. & Liu, R. (2020). Microstructure and synthesis mechanism of dysprosia-stabilized zirconia nanocrystals via chemical coprecipitation. *Ceramics International*. **46(9)**: 13331-13341.
- Li, Z., Liang, D., Zhong, C., Wan, T., Zhu, W., Luo, J., Yan, J. & Ren, F. (2025). Comprehensive evaluation of corrosion resistance and biocompatibility of ultrafine-grained TiMoNb alloy for dental implants. *Journal of Materials Science & Technology*. **221**: 247-259.
- Liu, J., Song, J., Qi, T., Zhang, C. & Qu, J. (2016). Controlling the formation of $\text{Na}_2\text{ZrSiO}_5$ in alkali fusion process for zirconium oxychloride production. *Advanced Powder Technology*. **27(1)**: 1-8.

- Luo, H., Wu, Y., Diao, X., Shi, W., Feng, F., Qian, F., Umeda, J., Kondoh, K., Xin, H. & Shen, J. (2020). Mechanical properties and biocompatibility of titanium with a high oxygen concentration for dental implants. *Materials Science and Engineering: C*. **117**: 111306.
- Maryani, E., Kurniasih, S.C., Sofiyarningsih, N. & Priyanto, B. (2018). Penyiapan komposit hidroksiapatit-zirkonia sebagai bahan biokeramik. *Jurnal Keramik. dan Gelas Indonesia*. **27(1)**: 40-50.
- Mobarak, M.B., Uddin, M.N., Chowdhury, F., Hossain, M.S., Mahmud, M., Sarkar, S., Tanvir, N.I. & Ahmed, S. (2024). Solid-state synthesis of poultry waste derived hydroxyapatite: Effect of calcination temperature on crystallographic parameters and biomedical competency. *Journal of Molecular Structure*. **1301**: 137321.
- Mohan, N., Palangadan, R., Fernandez, F.B. & Varma, H. (2018). Preparation of hydroxyapatite porous scaffold from a 'coral-like' synthetic inorganic precursor for use as a bone substitute and a drug delivery vehicle. *Materials Science and Engineering: C*. **92**: 329-337.
- Noviyanti, A.R., Akbar, N., Deawati, Y., Ernawati, E.E., Malik, Y.T. & Fauzia, R. P. (2020). A novel hydrothermal synthesis of nanohydroxyapatite from eggshell-calcium-oxide precursors. *Heliyon*. **6(4)**: 14859-14866.
- Septawendar, R. & Maryani, E. (2020). Sintesis bahan monoklinik zirkonia berukuran nano dari aprekursor zirkonium klorida menggunakan templat polietilen glikol. *Chimica et Natura Acta*. **8(1)**: 17-25.
- Septawendar, R., Nuruddin, A., Sutardi, S., Asri, LATW, Maryani, E., Ridwan Setiawan, A., & Sunendar Purwasasmita, B. (2019). Synthesis of one-dimensional ZrO₂ nanomaterials from Zr(OH)₄ precursors assisted by glycols through a facile precursor-templating method. *Materials Research Express*. **6(6)**: 65037.
- Veluswamy, R., Balasubramaniam, G., Natarajan, M., Krishnaswamy, M., Chinnappan, B. A., Nagarajan, S., Subramanian, B. & Velauthapillai, D. (2024). Multifunctional and sustainable hydroxyapatite from natural products for biomedical and industrial applications - A comprehensive review. *Sustainable Chemistry and Pharmacy*. **41**: 101653.
- Yılmaz, E. & Çalışkan, F. (2022). A new functional graded dental implant design with biocompatible and antibacterial properties. *Materials Chemistry and Physics*. **277**: 125481.
- Zheng, E., Feng, G., Jiang, F., Shao, C., Fu, H., Hu, Z., Wu, Q., Yang, Q. & Liu, J. (2024). Effect of process parameters on the synthesis and lead ions removal performance of novel porous hydroxyapatite sheets prepared via non-aqueous precipitation method. *Ceramics International*. **50(7)**: 10897-10905.
- Zhou, D., Ding, C., Han, W., Li, H., Zhang, H., Xu, W. & Zhou, Y. (2024). Low-temperature fabrication of zirconia transparent ceramics via hydrothermal nanopowder. *Ceramics International*. **50(23)**: 49210-49216.